Muon spin relaxation study of superconducting $Bi_2Sr_{2-x}La_xCuO_{6+\delta}$

P. L. Russo,* C. R. Wiebe,† and Y. J. Uemura‡
Department of Physics, Columbia University, New York, New York 10027, USA

A. T. Savici
Department of Physics, Columbia University, New York, New York 10027, USA
and Brookhaven National Laboratory, Upton, New York, New York 11973, USA

G. J. MacDougall, J. Rodriguez, and G. M. Luke
Department of Physics and Astronomy, McMaster University, Hamilton, Ontario, Canada, L8P 4N3

N. Kaneko,§ H. Eisaki,‖ and M. Greven
Deptartment of Applied Physics, Stanford University, Stanford, California 94305, USA

O. P. Vajk
NIST Center for Neutron Research, Gaithersburg, Maryland 20899, USA

S. Ono and Yoichi Ando
Central Research Institute of Electric Power Industry (CRIEPI), 2-11-1 Iwado Kita, Komae, Tokyo 201-8511, Japan

K. Fujita, K. M. Kojima, and S. Uchida
Department Physics, University of Tokyo, Tokyo 113-8656, Japan

(Received 8 February 2006; revised manuscript received 14 December 2006; published 15 February 2007)

We have performed transverse-field (TF) and zero-field (ZF) μSR measurements of $Bi_2Sr_{2-x}La_xCuO_{6+\delta}$ (Bi2201) systems with $x=0.2$, 0.4, 0.6, and 1.0, using ceramic specimens with modest c-axis alignment and single-crystal specimens. The absence of static magnetic order has been confirmed in underdoped ($x=0.6$) and optimally doped ($x=0.4$) systems at $T=2$ K, while only a very weak signature towards static magnetism has been found at $T=2$ K in the $x=1.0$ system, which is a lightly hole-doped nonsuperconducting insulator. In the superconducting ($x=0.6$, 0.4, and 0.2) systems, the relaxation rate σ in TF-μSR, proportional to n_s/m^* (superconducting carrier density and effective mass), followed a general trend found in other cuprate systems in a plot of T_c vs $n_s/m^*(T\rightarrow 0)$. Assuming the in-plane effective mass m^* for Bi2201 to be comparable to three to four times the bare electron mass m_e as found in $La_{2-x}Sr_xCuO_4$ (LSCO) and $YBa_2Cu_3O_{7-\delta}$ (YBCO) systems, we obtain $n_s\sim 0.15-0.2$ per Cu for the $x=0.4$ Bi2201 system. This carrier density is much smaller than the Hall number $n_{Hall}\sim 10$ per Cu obtained at $T<1.6$ K in high magnetic fields (40–60 T) along the c axis applied to suppress superconductivity. The present results of the superfluid density (n_s/m^*) in Bi2201 are compared with those from other cuprate systems, including YBCO systems with very much reduced $T_c<20$ K studied by microwave, H_{c1}, and inductance methods. Additional muon-spin-relaxation (μSR) measurements have been performed on a single-crystal specimen of Bi2201 ($x=0.4$) in a high transverse magnetic field of 5 T parallel to the c axis, in order to search for the field-induced muon spin relaxation recently found in LSCO and some other high-temperature superconducting cuprate (HTSC) systems well above T_c. The nearly temperature-independent and very small relaxation rate observed in Bi2201 above T_c rules out a hypothesis that the field-induced relaxation is directly proportional to the magnitude of the Nernst coefficient, which is a measure of the strength of dynamic superconductivity. We also describe a procedure for angular averaging of σ in μSR measurements using ceramic specimens with modest alignment of c-axis orientations, together with the neutron-scattering results obtained for determining the orientation distribution of microcrystallites in the present ceramic specimens.

DOI: 10.1103/PhysRevB.75.054511 PACS number(s): 74.62.−c, 74.72.Hs, 76.75.+i

I. INTRODUCTION

Mechanisms for superconductivity in high-temperature superconducting cuprate (HTSC) systems continue to be a subject of extensive study in condensed-matter physics. A search for the primary factors which determine the transition temperature T_c would be a promising route to solve this problem. In this spirit, we have accumulated muon-spin-relaxation (μSR) results of the magnetic-field penetration depth λ in various HTSC systems.[1,2] We have reported nearly linear correlations between T_c and n_s/m^* (superconducting carrier density and effective mass) in several cuprate systems with simple hole doping,[3,4] (Cu,Zn) substitutions,[5] partial volume having static incommensurate magnetic order,[6,7] and overdoping.[8,9] These results are consistent with other reports using μSR,[10–15] and other methods[16] in various cuprate systems. The linear relationship between T_c and the

superfluid density, combined with the pseudogap behavior, has been discussed as an essential element in several models for the cuprates, such as Bose-Einstein to BCS crossover,[17–21] holon Bose condensation in the *t-J* model,[22,23] boson-fermion models,[24,25] superconducting phase fluctuations,[26,27] and critical behavior in *X-Y* models.[28–30]

Following the series of measurements of dc conductivity in high magnetic fields by Ando, Boebinger, and co-workers,[31–33] Balakirev *et al.*[34] performed measurements of the Hall effect in $Bi_2Sr_{2-x}La_xCuO_{6+\delta}$ (Bi2201) systems by suppressing superconductivity with the application of high external magnetic fields along the *c* axis. Their results are rather surprising in that (i) the normal-state carrier concentration n_{Hall} at $T\rightarrow 0$ increases up to approximately one hole per Cu in the region near the optimal T_c, in contrast to the widely assumed carrier density of 0.15–0.2 holes per Cu in that region; (ii) n_{Hall} increases rapidly with decreasing temperature below $T\sim 50$ K; and (iii) there is a nearly linear relationship between n_{Hall} at $T\rightarrow 0$ and T_c, which extends possibly to the overdoped region. Earlier reports of n_{Hall} (Ref. 35) have been limited only to $T>T_c$ at low fields, and thus could not have revealed these anomalous features.

In order to distinguish whether or not this behavior of n_{Hall} is due to some special feature of the Bi2201 systems, we have performed μSR measurements of the superfluid density in Bi2201, and report the results in this paper. Our results from Bi2201 follow the general trend found in most other cuprate systems in the plot of T_c vs n_s/m^*. This implies that the anomalously large n_{Hall} should not be ascribed as a feature specific to the Bi2201 system.

Unlike most of the prototypical cuprate systems which have an average interlayer spacing of $c_{int}\sim 6$ Å between the CuO_2 planes, the Bi2201 systems have about a factor of 2 larger interlayer spacing, $c_{int}=12.3$ Å, similar to $Ta_2Ba_2CuO_{6+\delta}$ (Tl2201) with $c_{int}=11.6$ Å. Comparing the μSR results from systems with different interlayer spacings, we will discuss the relationship of two-dimensional (2D) and 3D superfluid densities with respect to T_c, and discuss if these and some other factor(s) play a primary role in determining T_c.

The Bi2201 series has T_c's of about 30 K in the optimally doping region. One of our specimens in the underdoped region has a substantially reduced $T_c\sim 12$ K, yet without static magnetic order down to $T=2$ K. Several reported studies on phase diagrams[36,37] indicate that Bi2201 systems exhibit a relatively smaller insulating region compared to $La_{2-x}Sr_xCuO_4$ (LSCO) systems,[33] as illustrated in Fig. 1. This feature makes Bi2201 attractively unique among the cuprate systems, distinguished by presumably the smallest tendency towards competing magnetic order.

Recently, extensive experimental studies have been made to measure the penetration depth λ in the very underdoped $YBa_2Cu_3O_{7-\delta}$ (YBCO) system with reduced $T_c<20$ K. These studies use a mutual inductance technique with YBCO thin films,[40] as well as magnetization measurements on H_{c1} (Ref. 38) and microwave absorption[39] on single-crystals specimens. Such underdoped YBCO systems, however, may have part of the volume undergoing static magnetic order, as reported by a recent μSR study.[41] In some underdoped LSCO systems and oxygen doped $La_2CuO_{4+\delta}$ (LCO) at low

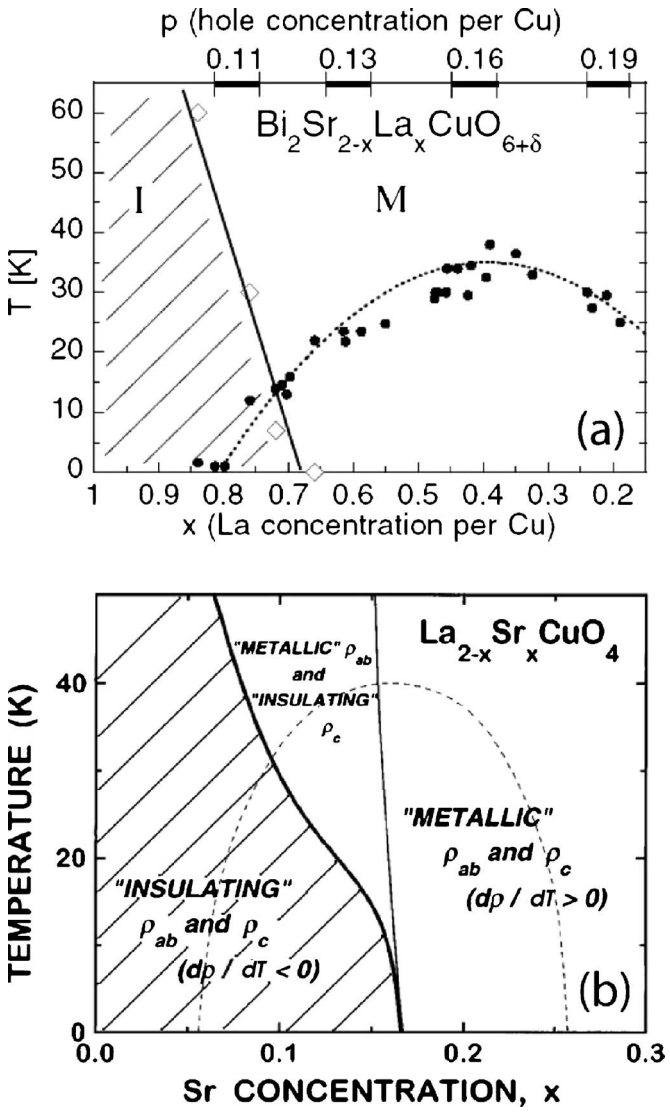

FIG. 1. Comparison of phase diagrams, obtained from transport measurements in high magnetic fields up to 60 T applied parallel to the *c* axis, for (a) Bi2201 (Ref. 36) and (b) LSCO (Ref. 33). In the shaded region, the in-plane conductivity (of Bi2201) and in- and out-of-plane conductivity (of LSCO) show an insulating behavior. Bi2201 has much smaller insulating region compared to LSCO.

temperatures, we found a microscopic separation of volume into small island regions with static magnetic order without superfluid and the remaining superconducting volume without static magnetism.[6,7] Contrary to these LSCO and YBCO systems, Bi2201 allows us to study the superfluid density of HTSC systems with very low T_c, free from the possible effects of coexisting magnetic volume fraction. With this feature in mind, we will compare our results of superfluid density in Bi2201 with published results in very-underdoped YBCO.

In derivation of the absolute values of λ and n_s/m^* from the μSR relaxation rate σ observed in transverse external fields, one needs to adopt a proper procedure for averaging over the orientation of microcrystallites in ceramic specimens, and also needs to ensure that the results are not affected by possible formation of 2D pancake vortices in high

fields.[42–44] In the present study, we have made an effort to elucidate these procedures by taking neutron scattering data for the distribution of crystal orientations, and by comparing the field dependence of σ and the Fourier-transform line shapes between the cases with single-crystal and ceramic specimens.

In μSR measurements with high transverse external magnetic fields up to 6 T applied parallel to the c axis, we[45] recently found a remarkable field-induced relaxation well above T_c and the magnetic ordering temperature T_N in several specimens of superconducting $(La_{2-x}Sr_x)CuO_4$ (LSCO), $(La_{2-x}Ba_x)CuO_4$ (LBCO), and $(La_{2-x-y}Sr_xEu_y)CuO_4$ (LESCO). There are two possible ways to interpret these results: (i) the external field changes the free energy balance between the superconducting state and competing magnetic state, favoring the latter and inducing static spin polarization as the effect of a cross term in free energy involving a product of superconducting and magnetic order parameters; (ii) a dynamic superconductivity above T_c,[1,50] observed via the Nernst effect,[46–48] causes a partial screening of the applied field,[49] leading to a field inhomogeneity analogous to that observed below T_c. Since Bi2201 is much less "magnetic" than LSCO and LBCO systems, comparison of field-induced effects between Bi2201 and the 214 systems might help in distinguishing these two scenarios. With this motivation, we performed μSR measurements on Bi2201 (x=0.4) applying a transverse field of 5 T. We observed nearly temperature-independent and very small relaxation above T_c, i.e., no field-induced effect has been detected. With some constraints, this result favors scenario (i) over (ii).

This paper is organized in the following way. We will first describe technical aspects about μSR measurements[51–55] and sample preparations in Sec. II. Section III will show μSR results in ceramic specimens of Bi2201 systems in zero field (ZF) and a transverse field (TF) of 200 G. Section IV will show the field dependence of σ and the line shapes in ceramic and single-crystal specimens, as well as the TF-μSR results in a high field of 5 T. Neutron studies of the orientation distribution will be shown in Sec. V, together with a discussion of procedures for angular averaging, to compare the present results with published results from single crystals and/or completely random ceramic specimens. In Sec. VI, we will compare our results with previous μSR results from various HTSC systems, as well as with recent inductance, microwave, and H_{c1} measurements. Finally, we will compare n_{Hall} and n_s, consider the primary factor which determines T_c, discuss the implications of the absence of the field-induced relaxation in Bi2201, and summarize the results from present studies in Sec. VII.

II. EXPERIMENTAL METHODS

A. μSR

The present μSR measurements were performed at the M20 beamline at TRIUMF, the Canadian National Laboratory located in Vancouver, Canada, which can provide a highly intense, polarized beam of positive muons. In transverse-field (TF) μSR measurements, the polarization direction of the in-flight muons is spin rotated via crossed electric and magnetic fields using a Wien filter, so their initial polarization becomes perpendicular to the field and beam direction. In contrast, zero-field (ZF) μSR measurements are usually performed with the muon polarized along its flight direction.

After implantation, the muon stops at an interstitial site, where the electrostatic potential energy has a minimum, within a time scale of typically less than 1 ns,[56] much shorter than the muon lifetime τ_μ=2.2 μs. In cuprate systems below about T=200 K,[57] an implanted muon is considered to rest at the interstitial site until its decay without being involved in a hopping motion.

We performed TF-μSR measurements by applying transverse external magnetic field of 50 G to 5 T parallel to the beam direction. TF-μSR allows us to measure the field distribution of the flux vortex lattice of type-II superconductors.[58] ZF-μSR would allow detection of spontaneous static magnetic order. The specimens were mounted in a He gas flow cryostat with the disc face (or ab-plane crystal mosaic face) perpendicular to the muon beam direction, along which the transverse external magnetic field was applied. Further details of the μSR technique can be found elsewhere.[54,55,58]

B. Preparation of specimens

Ceramic specimens of $Bi_2Sr_{2-x}La_xCuO_{6+\delta}$ (Bi2201) were prepared in a method similar to the crystal growth described in Ref. 59. Raw powders of Bi_2O_3, $SrCO_3$, La_2O_3, and CuO, with purities of 99.9% or higher, are dried, weighed, mixed into the nominal molar ratio of the target composition, and well ground in an agate mortar; they are then calcined at 750–850 °C for 20 h to form the Bi2201 phase. The resulting powders are reground and calcined again, and this process is repeated twice. The x-ray-diffraction analysis reveals that the powders become 100%-pure Bi2201 phase after the third calcination. The resulting Bi2201 powders are isostatically pressed into a small disc shape and finally sintered at 850 °C for 20 h, to form the polycrystalline specimens used for the present study. We have studied several specimens with different concentrations, covering the very-underdoped and nonsuperconducting region (x=1.0), as well as the underdoped (x=0.6), optimally doped (0.4), and overdoped (0.2) regions. The hard pressing before heat treatment caused a modest natural alignment of the ab-plane directions with respect to the surfaces of the disc-shaped pellet specimens, as described later.

We used a single crystal of $Bi_2Sr_{1.6}La_{0.4}CuO_{6+y}$ grown at Stanford University and another crystal of the same composition grown at University of Tokyo. The crystal growth and characterization of the former crystal is described by Eisaki *et al.*[60] In the following, we describe the growth and characterization method used at University of Tokyo, which is similar to the one used at Stanford University. The crystals were grown by using the traveling-solvent floating zone method in one atmosphere oxygen gas. All of single crystals were annealed at 650 °C for 48 h before subsequent quenching to room temperature. This procedure makes the oxygen distribution uniform. Temperature dependences of the magnetic

susceptibility, resistivity, and Hall coefficient were measured and published in Ref. 61. The transition temperature T_c, determined by the susceptibility, was 34 K, with a transition width of less than 3 K, which confirms the uniformity of the sample and its oxygen distribution. The Hall coefficient and the in-plane resistivity tangent of the Bi2201 crystal indicate that the average carrier concentration is at nearly optimum doping.

III. RESULTS FROM μSR MEASUREMENTS

A. ZF μSR

In order to check for the existence of static magnetic order in our specimens, we performed zero-field μSR measurements. Figure 2(a) shows the relaxation function $G_z(t)$ multiplied by the initial asymmetry A, observed in zero field in a ceramic specimen of $Bi_2LaSrCuO_6$ ($x=1$) in the very underdoped region. According to the phase diagram in Fig. 1(a), this concentration corresponds to that of the "parent antiferromagnetic compound" La_2CuO_4 in the case of the LSCO systems. We have observed a slowly decaying Gaussian signal at $T=100$ K, characteristic of systems without static magnetic order. The slow decay is due to nuclear dipolar fields. With decreasing temperature, we found a small increase of relaxation, as shown in Fig. 2(a). For the comparison purposes, we also include the ZF-μSR spectrum observed in La_2CuO_4, in which Cu moments of $\sim 0.4\mu_B$ order antiferromagnetically below $T\sim 250$ K (the Néel temperature depends strongly on oxygen composition[62]). Figure 2(a) demonstrates that the $x=1$ Bi2201 system may be heading towards static magnetic order, but the ordering temperature is less than $T=2$ K. This could imply either of the following two cases: (i) the tendency towards static magnetic order in the parent compound of Bi2201 is much weaker than in La_2CuO_4; or (ii) the carrier density in the nominally undoped Bi2201 is significantly higher than that of La_2CuO_4.

We have also performed ZF-μSR measurements on the superconducting Bi2201 ceramic specimens with $x=0.6$ and 0.4, comparing the spectra above T_c and at $T=2$ K. As shown in Fig. 2(b), these superconducting samples show a slow Gaussian decay of $G_z(t)$, without temperature dependence. Although we have not performed ZF-μSR measurements in the overdoped $x=0.2$ sample, the overdoped region in cuprate systems are considered to be free from static magnetism, based on experimental results from Tl2201 systems.[8] These results indicate that there is no detectable static magnetism developing in the superconducting specimens of Bi2201 reported in the present paper. All the temperature dependences of the relaxation rate observed in TF-μSR below T_c in such specimens should then be attributed to an inhomogeneous field originating from the flux vortices of the superconducting state.

B. TF μSR

Figure 3 shows the oscillating asymmetry $A(t) \equiv AG_x(t)\cos(\omega t+\phi)$ observed in the ceramic specimen of Bi2201 with $x=0.4$. The frequency ω is given by the product of the applied external field B_{ext} and the gyromagnetic ratio

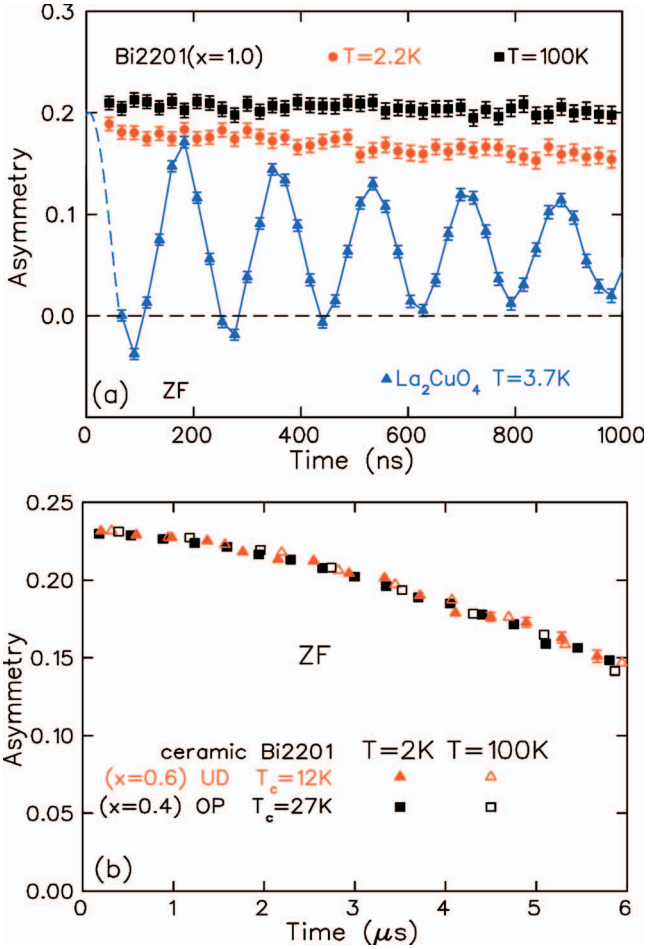

FIG. 2. (Color) Asymmetry $AG_z(t)$ of ZF-μSR time spectra observed in (a) a ceramic specimens of $Bi_2Sr_{2-x}La_xCuO_{6+\delta}$ (Bi2201) with $x=1$ (nonsuperconducting and nominally undoped parent compound) at $T=100$ and 2.2 K, and ceramic specimen of La_2CuO_4; and (b) in ceramic specimens of superconducting Bi2201 with $x=0.6$ (underdoped, $T_c=12$ K) and $x=0.4$ (optimally doped, $T_c=27$ K) at $T=2$ and 100 K.

$\gamma_\mu = 2\pi \times 13.56$ kHz/G of the muon spin. In the normal state above T_c, we see only a very slow damping of the precession signal, due to nuclear dipolar fields. However, after field cooling the system into the superconducting state in B_{ext}, we found that the asymmetry exhibits a clear damping. This damping is due to the inhomogeneous field from the flux vortex lattice.

For ceramic specimens, we usually approximate the relaxation function with a Gaussian decay,

$$G_x(t) = \exp(-\sigma^2 t^2/2), \tag{1}$$

and derive the muon-spin-relaxation rate σ. Nuclear dipolar relaxation can be subtracted in quadrature using the formula

$$\sigma_{sc} = \sqrt{\sigma^2 - \sigma_{nd}^2}, \tag{2}$$

where σ_{sc} is due to the superconducting vortex lattice and σ_{nd} is due to the nuclear dipolar fields. One can determine σ_{nd} by performing TF-μSR measurements in the normal state above T_c. Note that this correction procedure with Eq.

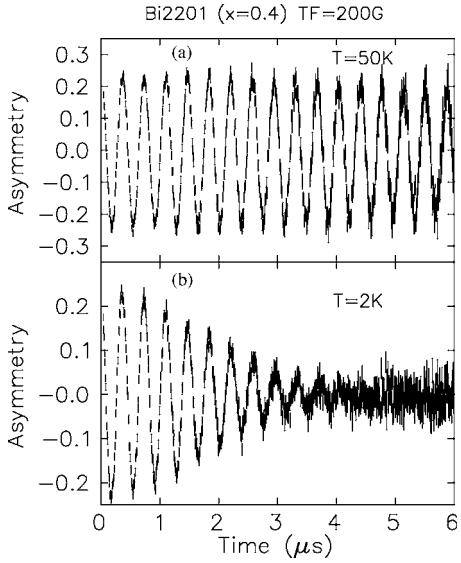

FIG. 3. Time spectra $AG_x(t)\cos(\omega t)$ observed in transverse-field μSR measurements in a ceramic specimen of Bi2201 (x=0.4) with B_{ext}=200 G at (a) T=50 K and (b) T=2 K. (b) Taken after field cooling in 200 G.

(2) causes large error bars around $T=T_c$. In the following, we will denote the corrected relaxation rate σ_{sc} simply by σ, unless stated otherwise.

Figure 4 shows the temperature dependences of the relaxation rate σ observed in ceramic specimens of Bi2201 with x=0.2,0.4,0.6, respectively, in the overdoped, optimally doped, and underdoped region, in a TF of 200 G. σ shows a rapid increase with decreasing temperature below T_c.

The relaxation rate σ in type-II superconductors is proportional to the width ΔH of the field distribution in the sample which is related to the penetration depth λ as

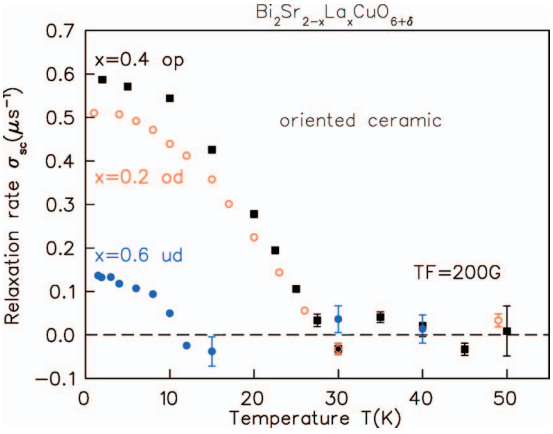

FIG. 4. (Color) Temperature dependence of the muon-spin-relaxation rate σ_{sc} due to superconductivity, observed in transverse-field μSR in B_{ext}=200 G in ceramic specimens of Bi2201 with x=0.6 (underdoped), 0.4 (optimally doped), and 0.2 (overdoped). The background relaxation rate due to nuclear dipolar fields σ_{nd}, estimated by averaging the observed relaxation rate σ above T_c, is subtracted quadratically following Eq. (2). Negative values of σ_{sc} indicate cases with $\sigma \leqslant \sigma_{nd}$.

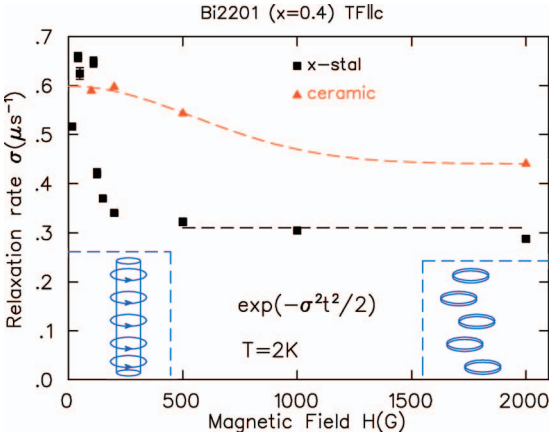

FIG. 5. (Color) Field dependence of the muon-spin-relaxation rate σ observed in transverse magnetic field in single-crystal and modestly oriented ceramic specimens of optimally doped Bi2201 (x=0.4) at T=2 K. The contribution from the nuclear dipolar field is not subtracted. The flux vortex has 3D structure in lower fields, and the 2D pancake structure in higher fields, as illustrated.

$$\sigma \propto \Delta H \propto 1/\lambda^2 = \frac{4\pi n_s e^2}{m^* c^2} \times \frac{1}{1+\xi_{ab}/l}, \tag{3}$$

where n_s denotes the superconducting carrier density and m^* is the effective mass. In the clean limit, where the mean free path l is much greater than the in-plane coherence length ξ_{ab}, Eq. (3) gives a simple relationship

$$\sigma \propto 1/\lambda^2 \propto n_s/m^*. \tag{4}$$

The parameter n_s/m^*, which is often referred to as the "superfluid density," is due to the density of the supercurrent which partially screens the external field B_{ext}. The results in Fig. 4 indicate that the underdoped Bi2201 system with x=0.6 has a much smaller superfluid density at $T\rightarrow 0$ compared to the optimally doped x=0.4 system with higher T_c.

IV. FIELD DEPENDENCE OF THE μSR RESULTS

A. Low-field region below 2 kG

In highly two-dimensional (2D) $Bi_2Sr_2CaCu_2O_8$ (Bi2212) superconductors, a strong reduction of the relaxation rate σ with increasing field was observed in the range of B_{ext}=400–600 G in TF-μSR measurements on single-crystal specimens with the external field B_{ext} applied parallel to the c axis.[42,43] This field dependence has been attributed to the formation of 2D pancake vortices in higher fields.[43] As illustrated in Fig. 5, the random location of vortex cores on different CuO_2 planes of the 2D vortex lattice would average (narrow) the width of the field distribution due to random location of vortex cores.

To examine this effect in Bi2201, we performed TF-μSR measurements of σ in field-cooled conditions at T=2 K in B_{ext}=50–2000 G using single-crystal and ceramic specimens with x=0.4 in the optimal doping region. In Fig. 5, we compare the field dependences of σ in the single-crystal (black symbol) and ceramic (red symbol) specimens. The results from the single-crystal specimen show a very

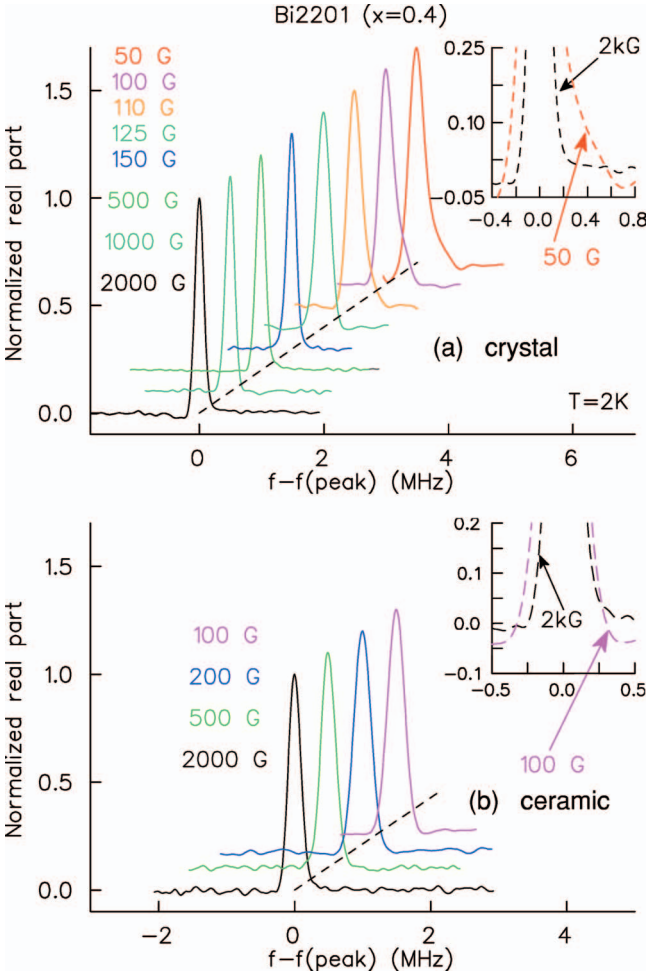

FIG. 6. (Color) Line shapes of Fourier-transformed spectra of transverse-field μSR in (a) a single-crystal specimen and (b) a mildly oriented ceramic specimen of optimally doped Bi2201 ($x=0.4$) observed at $T=2$ K in a few different values of external field. Asymmetric line shapes due to the internal-field profile of the 3D Abrikosov flux vortex lattice are seen in the results for the single-crystal sample in a low-field region.

sharp reduction at $B_{ext} \sim 100$ G with increasing field, followed by a saturation with an almost field-independent value of σ in higher fields. In contrast, the ceramic results show a much more gradual reduction of σ with increasing B_{ext}.

The change from 3D to 2D flux vortex lattice is associated with a change from an asymmetric to a more symmetric field distribution close to Gaussian in shape. This change has previously been studied in terms of the "skewness" of the line shape.[44] Here, we present this feature more directly by displaying the field distribution obtained via a Fourier transform of the precession signal. Figure 6 shows such line shapes in various fields for the case of single-crystal and ceramic specimens. The line shape from the single-crystal specimen shows a significant asymmetry in low fields, which becomes symmetric in higher fields. In contrast, the line shape from ceramic specimens is nearly symmetric in any field.

In earlier TF-μSR studies of superconducting YBCO, it has been observed[63] that the relaxation rate σ in unoriented ceramic specimens exhibits nearly no dependence on B_{ext} in

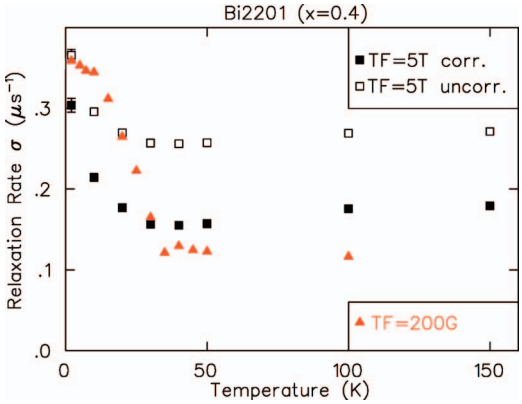

FIG. 7. (Color) Temperature dependence of the muon-spin-relaxation rate observed in transverse fields of 200 G and 5 T in a single-crystal specimen of optimally doped Bi2201 ($x=0.4$). The contribution from nuclear dipolar fields is not subtracted. The open-square results in 5 T include contributions from spatial inhomogeneity and drift of the applied field. The solid square symbols show the results after the correction for these applied-field effects.

a wide field range, typically $B_{ext}=500-4000$ G. This feature helps in comparisons of the results from various different measurements[8] in a plot of σ vs T_c, or σ vs composition. The tendency seen in Fig. 5 is consistent with this observation. A slow decay of the ceramic results with increasing B_{ext} may be attributed to (i) the stronger 2D character of Bi2201 with a wide separation of the adjacent CuO_2 planes of $c_{int}=12.3$ Å and (ii) a substantial alignment of the c axis caused by hard pressing, as described in the next section. These considerations suggest that a useful, risk-free method to measure σ in Bi2201 would be to study ceramic specimens with a relatively low B_{ext}, such as $B_{ext}=200$ G.

B. Searching for field-induced relaxation in high field up to 5 T

Motivated by our recent observation of a magnetic-field-induced muon-spin relaxation in LSCO and other cuprate systems above T_c,[45] we also performed TF-μSR measurements in an optimally doped Bi2201 ($x=0.4$) single crystal by applying an external field of 5 T parallel to the c axis. Figure 7 shows the temperature dependence of the relaxation rate σ observed in TF=5 T and 200 G. In high-field measurements, there is a relaxation caused by the spatial inhomogeneity and/or time-dependent drift of the external field. This effect was estimated by a μSR signal from a single crystal of $CaCO_3$, placed very close to the specimen. By a quadratic subtraction of the relaxation rate in $CaCO_3$ observed at 200 G from that at 5 T, we estimated the instrument-originated relaxation σ_{ins} to be 0.2 μs^{-1}. In Fig. 7, we also show the results in 5 T after the correction of this effect via quadratic subtraction.

We find nearly no temperature dependence of σ in 5 T above T_c. The value of $\sigma(T \to 0)=0.3$ μs^{-1} in 5 T, after the correction for σ_{ins}, is comparable to the low-field results shown in Fig. 5. The temperature dependence of the results

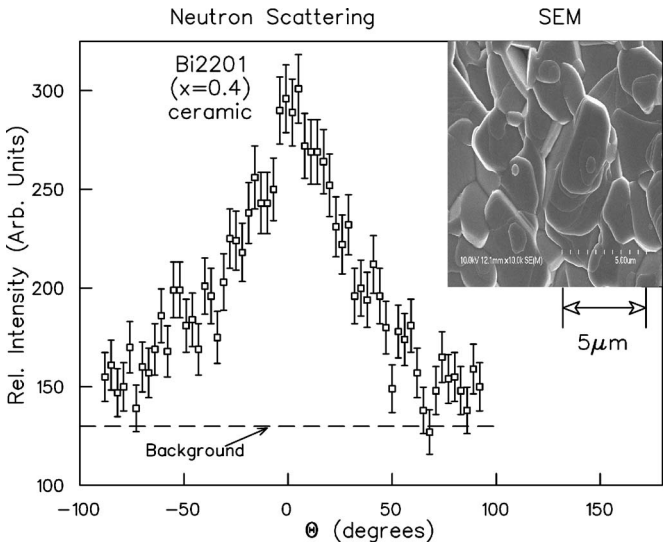

FIG. 8. Intensity profile, as a function of the angle θ between the line bisecting the scattering angle and the line normal to the sample disc surface, observed in a modestly oriented ceramic specimen of Bi2201 (x=0.4) by elastic neutron scattering at the setting of the scattering angle at that of the [006] Bragg reflection. The broken line shows the background contribution from nuclear incoherent scattering determined by setting the scattering angle off from the Bragg peak position. The inset figure shows the scanning electron microscope (SEM) image of grain size at the surface of the ceramic specimen of Bi2201 (x=0.4) used in the μSR and neutron measurements.

in 200 G below T_c follows the behavior expected for a d-wave superconductor with nodes in the energy gap.

V. CRYSTALLITE ALIGNMENT AND ANGULAR AVERAGING IN CERAMIC SPECIMENS

A. Neutron-scattering measurements

When one derives the penetration depth λ from the relaxation rate σ observed in ceramic specimens, it is very important to account for the effect of the distribution of crystallite directions. To estimate the alignment of the crystallites in our ceramic specimens, we carried out neutron-diffraction measurements at the BT2 beamline at the NIST Center for Neutron Research in Gaithersburg, MD. We obtained the angular dependence of the [006] Bragg scattering intensity as shown in Fig. 8, where the angle θ is defined as the angle between the vector normal to the disc surface and the direction bisecting the scattering angle. The background level (BG) from nuclear incoherent scattering, estimated at a slightly different momentum transfer, is indicated by the broken line.

The intensity profile exhibits a broad peak having a Gaussian width Δ_θ of ~26°–30° (full width at half maximum ~40–50), indicating that the present ceramic specimens have a modest alignment of the c-axis directions of their crystallites perpendicular to the disc surface. This width is comparable to those found with surface imaging by scanning electron microscopy (SEM) and x-ray diffraction of similarly prepared samples of $Bi_{2-x}Pb_xSr_2Ca_2Cu_3O_{10+y}$ (Bi2223) with a hard press of 6 kbar.[64] By fitting the intensity profile to a Gaussian function

$$P(\theta) \propto \exp(-\theta^2/2\Delta_\theta^2) + \mathrm{BG}, \tag{5}$$

we obtained Δ_θ=34°,26°,49°, for our ceramic specimens of x=0.2, 0.4, and 0.6, respectively. The intensity profile $P(\theta)$ is proportional to the probability of finding a crystallite, whose ab plane is perpendicular to the neutron-scattering plane, and the c-axis direction is off by the angle θ from the vector normal to the disc surface. The probablity to find a crystallite which satisfies the latter condition alone is proportional to $P(\theta)\sin(\theta)$.

B. Correction factors to the μSR data

Theoretical studies of Barthord and Gunn[65] and experimental studies of Forgan and co-workers[66] have shown that the μSR relaxation rate for single crystal or perfectly aligned ceramic specimens of highly anisotropic superconductors depends on the angle θ between the applied field and the c axis of the crystallite as

$$\sigma(\theta) \propto \frac{1}{\lambda_1\lambda_3}[\sin^2(\theta) + (\lambda_3/\lambda_1)^2\cos^2(\theta)]^{1/2}, \tag{6}$$

where λ_1 is the in-plane penetration depth and λ_3 is the out-of-plane penetration depth.

Our sample can be thought of as a large collection of small single crystals. Note that the grain size shown in the inset of Fig. 8, 3–5 μm, is significantly larger than the in-plane penetration depth 0.3–0.5 μm and the intervortex distance 0.4 μm for B_{ext}=200 G. At a first glance, a quadratic angular average σ_{av} of $\sigma(\theta)$,

$$\sigma_{av}^2 = \frac{\int \sigma(\theta)^2 P(\theta)\sin(\theta)d\theta}{\int P(\theta)\sin(\theta)d\theta}, \tag{7}$$

looks sufficient to account for the field width of ceramic specimens. However, there is an additional contribution coming from the spread of the "median" field, or in other words, the "shift" K, in different crystallites with different angle θ. The median field in each crystallite may be different from the macroscopic median field over the whole sample. Here, in view of Eq. (1) and associated arguments in Ref. 67 we will assume that the shift $K(\theta)$ of each crystallite is proportional to the width $\sigma(\theta)$, as $K(\theta)=C\sigma(\theta)$, where C is a proportionality constant.

The additional broadening of the field distribution comes not from the shift K itself, but from the *width* of K, which we denote as Δ_K. For example, for a single crystal placed at an angle θ, K is finite, but Δ_K=0, and therefore $\sigma(\theta)$ alone should represent the width. If there is a spread in effective demagnetization factor among crystallites,[68] that may also contribute to Δ_K. By using a relationship

$$\Delta_K^2 = \langle K^2\rangle - \langle K\rangle^2 = C^2[\langle\sigma^2\rangle - \langle\sigma\rangle^2], \tag{8}$$

where the symbol $\langle\ \rangle$ denotes an angular average, we can calculate Δ_K for any given distribution of $P(\theta)$. After this, we

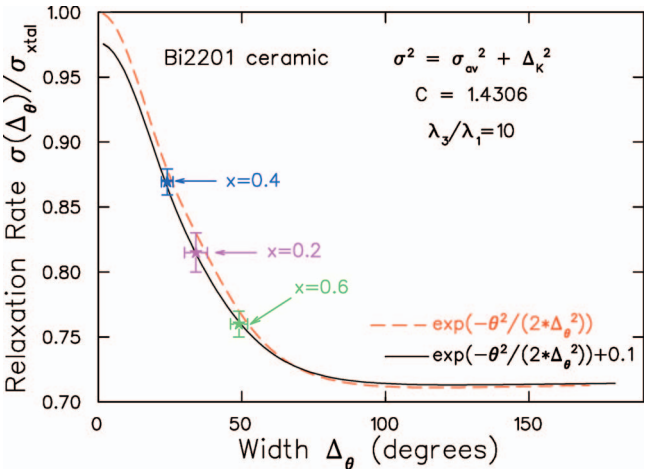

FIG. 9. (Color) Simulation results of the muon-spin-relaxation rate σ expected in oriented ceramic specimen with a Gaussian distribution of crystallite orientations [Eq. (5)] with the width Δ_θ calculated assuming a factor $C=1.43$ for the contribution of shift broadening in Eq. (8). The values of σ are normalized to σ_{xtal} expected for a single-crystal specimen. The results corresponding to the cases for Bi2201 specimens with $x=0.2$, 0.4, and 0.6 are shown, respectively, at their values of Δ_θ determined by neutron-scattering intensity (shown in Fig. 8 for the $x=0.4$ specimen).

should add this contribution, quadratically, to the width σ_{av} as

$$\sigma^2 = \sigma_{av}^2 + \Delta_K^2 \tag{9}$$

to obtain the actual relaxation rate σ.

For a given value of the factor C, one obtains a corresponding ratio between the single-crystal value $\sigma_{xtal} \equiv \sigma(\theta=0)$ and the relaxation rate expected for a ceramic sample with completely random crystal orientations, which we denote as a powder average value σ_{pwd}. For cuprate systems having a large anisotropy, we perform this calculation assuming $\lambda_3=10\lambda_1$ in Eq. (6), which represents the situation $\lambda_3 \gg \lambda_1$. Over 14 years, based on empirical checks of various results from YBCO specimens in randomly oriented ceramic, artificially oriented ceramic, and single-crystal specimens, we have adopted a correction factor $\sigma_{xtal}=1.4\sigma_{pwd}$ (we first adopted this factor in 1991 in Ref. 4 on p. 2666). This ratio is obtained for $C=1.4306$. Therefore we proceed with our calculation using this value for the factor C. In the next section, we shall see that μSR results obtained in ceramic and single-crystal specimens of YBCO systems with $T_c \sim 60$ K become consistent with each other if one uses this conversion factor.

We have calculated the relaxation rate σ for a Gaussian distribution of $P(\theta)$ as a function of the width Δ_θ, and show the results in Fig. 9. The broken red line shows the case for a Gaussian $P(\theta)$ while the solid line for Gaussian plus a constant background of 10% of the peak height, which corresponds to the situation shown in Fig. 8. The width Δ_θ for our Bi2201 specimens and the corresponding correction factors are shown by the colored symbols in this figure. This calculation suggests that we need to multiply the observed value of σ from the ceramic specimen with $x=0.4$ by a factor $0.71/0.86=0.83$ when we compare it with the results of unoriented random ceramic specimens. The magnitude of this correction is consistent with the experimental results of Bi2223 by Grynszpan *et al.*,[64] who found about ~20% increase of σ from low-texture (presumably nearly completely random in direction) to high-texture ceramic specimens which has a width Δ_θ comparable to that of the present Bi2201 ceramic specimens. In a similar procedure, we obtain the correction factor of $0.71/0.81=0.88$ and $0.71/0.76=0.93$, respectively, for the $x=0.2$ and 0.6 ceramic specimens.

VI. COMPARISON WITH SUPERFLUID DENSITY FROM OTHER SYSTEMS

To compare the present results of Bi2201 with the previous μSR results from other cuprate systems obtained using unoriented ceramic specimens, we multiplied the above-mentioned factors to σ obtained from Bi2201, and show them in a plot of $\sigma(T \to 0)$ vs T_c in Fig. 10(a). The points from Bi2201 systems (red square symbols) lie near the linear relationship from YBCO and other cuprate systems. For a more precise comparison, the low σ–low T_c region is expanded in Fig. 10(b). The points from Bi2201 lie significantly above the line extrapolated from μSR results on YBCO with higher T_c's, and the relative deviation becomes larger for systems with lower T_c.

In Fig. 10(b), we also include recent results on YBCO systems with rather low T_c's near the insulator-superconductor transitions, obtained using single-crystal specimens in microwave[39] and H_{c1} (Ref. 38) measurements, and thin-film specimens in inductance[40] measurements. For these YBCO results, we first converted the reported values of the *ab*-plane penetration depth λ [Å] into the μSR relaxation rate σ by using the relationship $\sigma\ [\mu s^{-1}]=(2700/\lambda)^2$ to get the value of σ expected for single crystals with B_{ext} parallel to the c axis. This conversion factor is given in Ref. 69, p. 606. To compare with the points in Fig. 10, we then need to convert into the corresponding powder value of σ by multiplying with a factor $1/1.4=0.71$.

By using these factors, we converted the penetration depth values obtained in μSR measurements of single crystals of $YBa_2Cu_3O_{6+\delta}$,[70–72] and plot them in Fig. 10(a) with the blue "dot in open circle" symbols. The excellent agreement of these points with the results from ceramic specimens of YBCO (black open circles) demonstrates that there is no contradiction between μSR results from single-crystal and ceramic specimens if these conversion factors are adopted.

Figure 10(b) shows that the results from microwave and H_{c1} on YBCO agree very well with each other, but the inductance results are very different, yielding about a factor ~5 smaller value of the superfluid density n_s/m^* for a system with comparable T_c. The disagreement between the inductance and microwave-H_{c1} results of YBCO may be ascribed to one or all of the following reasons: (i) the conversion factor from inductance to λ might involve a significant systematic error; (ii) the inductance measurement might be influenced by the c-axis penetration depth, which could give an apparently smaller superfluid density; (iii)

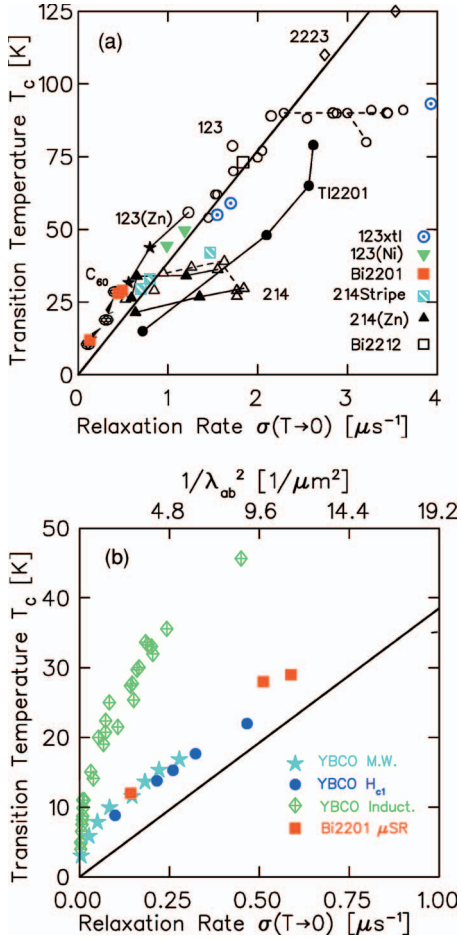

FIG. 10. (Color) Superconducting transition temperature T_c of HTSC and other type-II superconductors plotted against the muon-spin-relaxation rate $\sigma \propto n_s/m^*$ at $T \rightarrow 0$. (a) compares the present Bi2201 results with those of YBCO (open circle), LSCO (open triangle) and other cuprates (Refs. 2 and 3), Zn-doped cuprates (closed triangle) (Ref. 5), overdoped Tl2201 (closed circle) (Ref. 8), A_3C_{60} (Ref. 69), and LCO, LSCO (Ref. 6), and LESCO (Ref. 7) systems with partial volume having static stripe magnetic order (blue striped square). The blue "dot in open circle" points represent the μSR results of λ for single-crystal specimens of YBCO (Refs. 70–72), converted following the procedures in the text. An expanded plot in (b) compares the present μSR results on Bi2201 with the superfluid density n_s/m^* estimated in YBCO by microwave (Ref. 39) and H_{c1} (Ref. 38) measurements on single crystals and by inductance measurements (Ref. 40) on thin-film specimens.

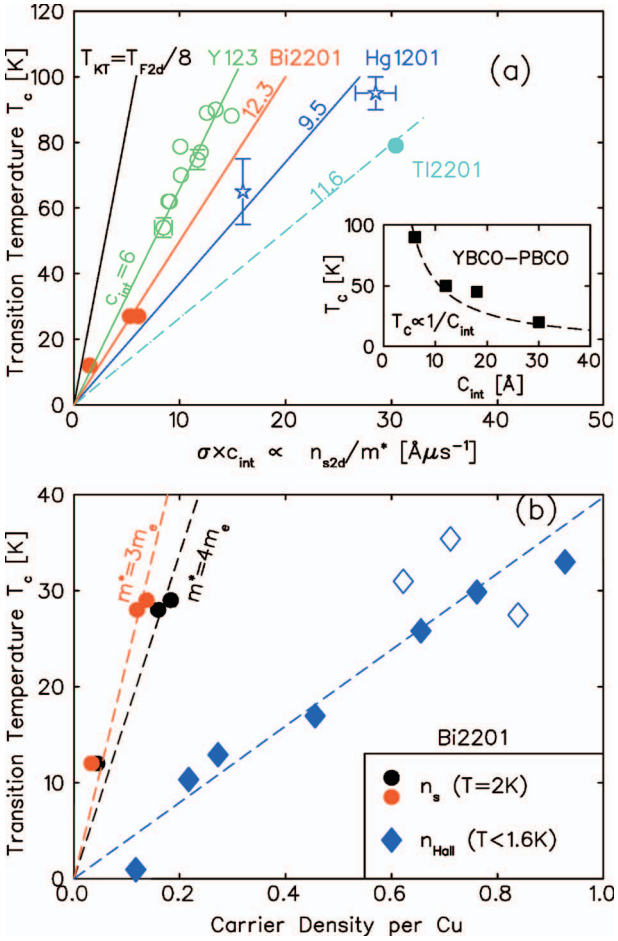

FIG. 11. (Color) (a) Transition temperature T_c of various HTSC systems plotted against the product of the muon-spin-relaxation rate $\sigma(T \rightarrow 0)$ and the average distance c_{int} of adjacent CuO_2 planes. The horizontal axis represents the 2D superfluid density n_{s2d}/m^*. The T_{KT} line shows system-independent superfluid density expected in the Kosterlitz-Thouless theory for purely 2D superfluid systems just below the transition temperature (Ref. 79). The inset shows the relationship between T_c and c_{int} obtained for MBE-made thin films of alternating layers of optimally doped YBCO and insulating PBCO ($PrBa_2Cu_3O_7$) stacked along the c-axis direction (Ref. 73). (b) A plot of T_c vs carrier density per Cu for Bi2201 obtained in the present work for the values of m^* estimated for YBCO and LSCO systems (Ref. 74), and the Hall number n_{Hall} obtained in the high-field Hall measurements (Ref. 34).

there may be a significant difference in the quality of single-crystal and thin film YBCO specimens. In Fig. 10(b), we also find that the points from the microwave and H_{c1} results of YBCO lie very close to the points from the present μSR results on Bi2201.

By multiplying σ with the interlayer distance c_{int} of different cuprates, we can obtain the 2D superfluid density n_{s2d}/m^*_{ab} on a CuO_2 plane. In this conversion, we count adjacent CuO_2 planes of double (triple) layer systems as two (three) independent conducting planes. Bi2201 has c_{int} =12.3 Å, which is about a factor 2 larger than $c_{int} \sim 6-7$ Å for LSCO and YBCO systems. Figure 11(a) shows a plot of T_c vs n_{s2d}/m^*_{ab}. Unlike in the 3D plot, we no longer see a nearly universal relationship. Systems with smaller c_{int} tend to have a higher T_c for a given 2D superfluid density n_{s2d}/m^*, although the results from Bi2201 and Tl2201 exhibit some scatter. An inverse correlation between T_c and c_{int} was found[73] in thin MBE films of a unit-cell-thick $YBa_2Cu_3O_7$ sandwiched with nonsuperconducting $PrBa_2Cu_3O_7$, as shown in the inset of Fig. 11(a).

VII. DISCUSSIONS AND CONCLUSIONS

A. Comparison with Hall number results

Figure 11(b) shows the results of Hall number n_{Hall} measurements of Bi2201,[34] given in the unit per Cu, at $T \rightarrow 0$ in

a very high magnetic field of up to 60 T applied perpendicular to the c axis of single-crystal specimens. As reported in Ref. 34 n_{Hall} exhibits a variation similar to that of n_s/m^* in Fig. 10, when plotted vs T_c. However, the absolute value of the carrier density ($n_{Hall} \sim 1$ per Cu in Bi2201 in the optimal doping region) is much higher than the commonly assumed carrier density of 0.15–0.2 holes per Cu in other cuprate systems in the optimal doping region.

Without having independent information on the effective mass m^*, it is not possible to make a direct comparison between the penetration depth results and the Hall number results, since the former represents n_s/m^* while the latter corresponds to the normal-state carrier density. Likewise, one needs to know possible system and doping dependences of m^* in order to compare n_s in different cuprate systems using the penetration-depth results. Recently, Padilla *et al.*[74] derived an in-plane effective mass m^*_{ab} in LSCO and YBCO systems from dc Hall effect results in relatively low fields above T_c and the spectral weight of optical conductivity. They obtained $m^* \sim 3-4m_e$, common to both systems and nearly independent of doping in a wide range from underdoped to optimally doping regions.

If we assume that m^* in Bi2201 is comparable to that in YBCO and LSCO systems, we can derive the superfluid density n_s from the penetration depth results. Figure 11(b) shows n_s of Bi2201, derived for the case of $m^*=3m_e$ and $4m_e$, compared with n_{Hall} in the plot of T_c vs carrier concentration per Cu. We clearly see a factor 4 or more difference in n_s and n_{Hall}. Carrier density in other systems, for the same effective mass, can be scaled using the results in Fig. 11(a), since the 2D carrier density is proportional to the density per Cu for most of the cuprate systems with nearly equal a- and b-axis lattice constants.

The results in Fig. 11 indicate that it is very difficult to expect an exceptionally high carrier density exclusively in Bi2201. The high Hall number n_{Hall} should not be attributed to a special difference of Bi2201 from other cuprate systems. Indeed, more recent studies of high-field Hall effect indicate that a comparable density $n_{Hall} \sim 1$ per Cu or even higher density has been also observed in LSCO systems near the optimum doping.[75] The very large value of n_{Hall} and its strong temperature dependence[34] remain to be explained in future investigations. We note that the Hall coefficient in the normal state is supposed to reflect the intrinsic Fermi-surface shape[76] in the zero-temperature limit, and hence is not necessarily a direct measure of the carrier number.

B. Correlations between σ and T_c

Since 1989, various discussions have been made on correlations between T_c and $\sigma \propto n_s/m^*$ based on the results shown in Fig. 10(a).[2,23,27] In this figure, we find a nearly linear correlations between T_c and the superfluid density in the underdoped region of YBCO and some other cuprate systems. The present results from Bi2201 roughly follow the general trend of other systems. On the other hand, this figure also shows that there are many cases in which the points deviate from the linear tendency. Most remarkable is the "plateau" region at T_c=90-K YBCO systems, which is due to the effect of superconductivity carried by the CuO chain.[12] The LSCO systems also exhibit a rather early "departure" from the linear relationship, whose possible implications will be discussed later.

Recently a power law different from the linear relationship has been obtained by the authors who reported the H_{c1},[38] microwave,[39] and inductance results[40] from YBCO systems having a rather reduced T_c, typically lower than 20 K. Indeed, the YBCO points in Fig. 10(b) exhibit a sublinear dependence of T_c on $n_s/m^*(T \rightarrow 0)$. In these reports, the T_c vs n_s/m^* plot is made with logarithmic scales, covering a wide temperature regions for T_c, and including results obtained from different methods. The power α of $T_c \propto (n_s/m^*)^\alpha$, derived in such a logarithmic plot would predominantly reflect the data obtained for YBCO systems with $T_c < 20$ K. Recent scanning tunnel microscopy (STM) measurements revealed that Bi2212 HTSC systems have a significant distribution of doping concentrations, and/or microscopic heterogeneity of electronic structures.[77,78] In general, a microscopic or macroscopic heterogeneity of the system would result in lower superfluid density for a given T_c, and such influence would be more severe for systems having lower T_c's, analogous to an effect of heterogeneity in percolation problems.

As exemplified by the large difference between H_{c1}-microwave data and the inductance data on YBCO low-T_c systems, a large systematic error can be involved in derivation of the superfluid density in different measurements. The statistical accuracy of μSR results on superfluid density is usually less than a few percent, which allows accurate comparisons of the relative change among data taken with equivalent conditions. Nevertheless, there exists room for a 10% or possibly even larger systematic uncertainties in the derivation of λ (or n_s/m^*) from σ, due to multiple possible choices in fitting functions of line shapes, assumptions for internal field distributions, method of angular averaging, etc.: see Secs. IV and V for details. Therefore comparisons among the superfluid density results from different methods should be done with an extra caution.

ZF-μSR measurements on YBCO and LSCO systems having rather reduced T_c's (Refs. 6 and 41) revealed the existence of a major volume fraction which has a static magnetic order. In the study of LESCO,[7] we found evidence that such a magnetic volume does not carry superfluid. These results imply that superconductivity of the very low-T_c YBCO systems survives on rather intricate paths of a minor volume fraction. The variation of T_c vs superfluid density in such a situation is certainly an interesting subject of research. However, it is highly questionable how much of the information from such systems can be used for discussing general and intrinsic properties of the cuprates.

The present results on Bi2201 systems have been obtained for specimens which do not involve static magnetic order. In this sense, they might represent an intrinsic property free from the possible complications due to magnetic volumes. Although within the above-mentioned limitations of comparing results from different methods, the good agreement of the present Bi2201 results and the YBCO results from H_{c1} and microwave measurements may support a view that the magnetism effect is not quite severe in YBCO systems with

lower T_c's. On the other hand, in such an argument based on results from different cuprate families, one has to check "universality" by adding data from a few more different systems. Based on these considerations, we show the results in the linear-scale plots of Figs. 10 and 11, without further processing the results nor deriving the "power."

In ceramic specimens of isotropic superconductors, the relaxation rate σ is nearly independent of B_{ext} used in TF-μSR measurements.[69] In modestly anisotropic YBCO systems, the relaxation rate in TF-μSR is nearly independent of the field both for measurements using ceramic[63] (for $B_{ext}=0.5-3$ kG) and single-crystal specimens[70] (for $B_{ext}<10$ kG). These features facilitated comparison of the results obtained with different B_{ext} in Fig. 10(a). The present study of the field dependence of σ, shown in Fig. 5, indicates that one has to use sufficiently low B_{ext} to assure the formation of a 3D vortex lattice in the case of highly anisotropic HTSC systems, such as Bi2201, even when ceramic specimens are used. This consideration suggests that some of the earlier μSR results on ceramic and powder specimens of highly anisotropic Bi2212 systems in $B_{ext}=3$ kG (Ref. 68) may involve a reduction of σ due to the possible formation of a 2D vortex lattice.

C. Primary factors which determine T_c

In 1995, Emery and Kivelson[27] discussed that the nearly linear relationship shown in Fig. 10(a) can be taken as a signature that the transition temperature T_c in HTSC systems is determined by phase fluctuations, i.e., an argument parallel to that of the Kosterlitz-Thouless (KT) transition in 2D systems. The KT theory[79] relates the 2D superfluid density n_{s2d}/m^* at $T=T_c$ and T_c with a system-independent universal relationship shown by the solid line T_{KT} in Fig. 11(a). As shown in this figure, the superfluid densities at $T\rightarrow 0$ in many HTSC systems are significantly higher than the density expected from the KT theory for a purely 2D system having the same T_c's. Furthermore, near T_c, the superfluid density becomes significantly less than that of the universal KT value in some HTSC systems, including the present Bi2201 and the YBCO systems studied by microwave and H_{c1} measurements.[38,39] These results, together with the strong dependence of T_c on c_{int}, indicate that the HTSC systems are substantially different from ideal 2D systems which undergo KT transition. These points are missed in the argument of Emery and Kivelson.

To account for any correlations between T_c and the superfluid density at $T\rightarrow 0$, it is very important to identify the process which reduces the superfluid density from the value at $T\rightarrow 0$ to the value near T_c. In general, the order parameter in superconductors and/or superfluids can be reduced in pair-breaking single-particle excitations across the gap and/or collective-mode excitations, such as rotons in superfluid ^{4}He. In the underdoped cuprates, the energy gap Δ, determined by tunneling or scanning tunneling microscope studies, decreases with increasing doping. Contrary to this, T_c increases with increasing doping. Due to this opposite behavior, it is difficult to ascribe T_c to pair-breaking excitations across Δ.

Recently, one of the authors[1,2] has proposed a view that the 41-meV magnetic-resonance mode observed by neutron scattering and the superconducting coherence peak (SCP) observed by angle resolved photo-emission spectroscopy (ARPES) experiments both represent spin and charge branches, respectively, of strongly coupled spin-charge excitations in cuprates, and this collective excitation plays a dominant role in the reduction of superfluid density in HTSC systems. Figure 12 shows a universal and nearly linear relationship between the energy of the magnetic-resonance mode,[80] Raman A_{1g} mode,[81] and the ARPES SCP (Ref. 82) vs T_c. In this type of collective-mode picture, the rather low T_c's in Bi2201 systems could be attributed to its low mode energy, shown in Fig. 12. Similarly, the early "branching off" of the LSCO systems from the linear line[3] in Fig. 10(a) could be attributed to the closeness of LSCO systems to the competing spin-charge modulated stripe state, which lowers the soft-mode energy.

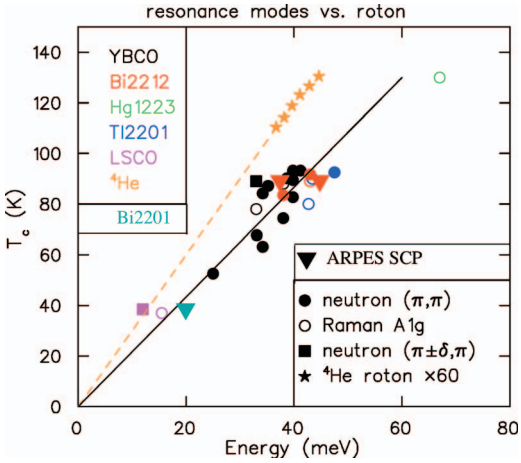

FIG. 12. (Color) Plot of T_c vs the energy of the roton minimum of bulk superfluid ^{4}He (values for both axes multiplied by a factor 60) measured under applied pressures (Ref. 83), compared with the relationship seen in HTSC systems for the energies of the neutron resonance mode at (π,π) (Ref. 80), the Raman $A1_g$ mode (Ref. 81), and the ARPES SCP (Ref. 82). Also included are the neutron energy transfers of spectral weight maximum near the $(\pi\pm\delta,\pi)$ point in YBCO (Ref. 80) and LSCO (Ref. 84) (closed squares). Taken from Uemura (Ref. 1).

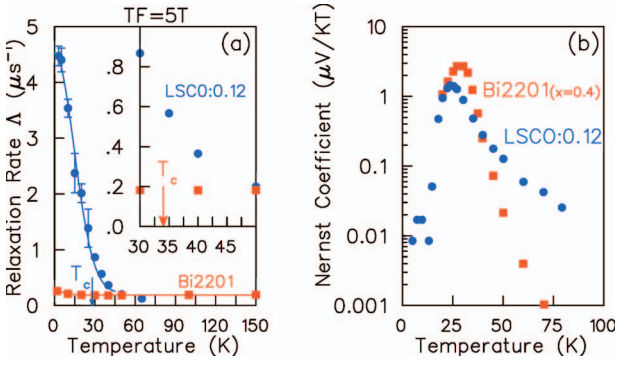

FIG. 13. (Color) Comparison of (a) the μSR and (b) the Nernst-effect results for optimally doped Bi2201 ($x=0.4$) and $La_{1.88}Sr_{0.12}CuO_4$ (LSCO:0.12). (a) shows the present results for Bi2201 and our recent results (Ref. 45) for LSCO:0.12 in TF-μSR with $B_{ext}=5$ T. (b) shows the Nernst coefficient (see text) in Bi2201 (Ref. 48) and LSCO:0.12 (Ref. 85).

Nernst effect measurements[46–48] have revealed a large region of "dynamic superconductivity"[1,50] due to phase fluctuations above T_c in several HTSC systems. The existence of phase fluctuations does not necessarily imply a KT transition as the sole factor which determines T_c. Collective modes, such as rotons, also cause decondensation of a condensate via phase fluctuations of otherwise coherent wave functions of condensed bosons. Further studies are, however, necessary to distinguish whether the single-particle or collective or both processes have a dominant role in the destruction of superfluid density in cuprate systems.

D. Field-induced relaxation above T_c and T_N

InTF-μSR measurements with a large external magnetic field up to 6 T applied parallel to the c axis, we recently found a field-induced muon-spin relaxation in several single-crystal specimens of LSCO, LBCO, and LESCO well above T_c and the magnetic transition temperature T_N.[45] The relaxation rate in the high-temperature region was proportional to the external field. In Fig. 13(a), we compare the relaxation rate observed in LSCO:0.12 with Sr concentration $x=0.12$ and the present results of Bi2201 ($x=0.4$), both obtained in TF=5 T. The LSCO results exhibit a strong temperature dependence, while the relaxation rate for Bi2201 is very small and shows nearly no temperature dependence above T_c, indicated by the arrows in the figure. As discussed in Sec. IV B, a significant part of the relaxation in Bi2201 comes from the field inhomogeneity and drift due to experimental instruments in high fields.

The induced voltage e_y of the Nernst effect, normalized to the temperature gradient, is nearly proportional to the applied field B in a region well below H_{c2}. The Nernst coefficient ν is defined as e_y/B. Figure 13(b) shows ν observed in LSCO:0.12 and Bi2201 ($x=0.4$).[48,85] Both of these systems exhibit a large Nernst effect of a similar magnitude and temperature dependence at $T\sim 40$ K just above T_c.

Recently, Ong and collaborators[49] reported a very small diamagnetic magnetization M_{dia} above T_c observed in Bi2212 systems in the region where the Nernst effect was also observed. The diamagnetic magnetization M_{dia} at $T>T_c$ scales with ν in Bi2212. If we assume that this feature can be extended to the cases in LSCO:0.12 and Bi2201, with a comparable magnitude of the proportionality constant between M_{dia} and ν, we can expect M_{dia} for these two systems to be comparable in magnitude at $T=30-50$ K.

The μSR relaxation rate in these two systems are very different at $T=30-50$ K. This contrast suggests that the field-induced relaxation above T_c may not be caused by the diamagnetic magnetization M_{dia}. As discussed in Sec. I, Bi2201 has much smaller tendency towards magnetic order compared to LSCO systems. The marked difference in the field-induced effect in Fig. 13 suggests that this effect may be related to the closeness of the superconducting state to the competing magnetic state, in free energy and/or doping composition range.

E. Summary

In this paper, we have reported TF- and ZF μSR measurements of modestly oriented ceramic and single-crystal specimens of Bi2201 systems. We found that n_s/m^* at $T\rightarrow 0$ in Bi2201 systems follows a general trend of other cuprates in the plot of T_c vs n_s/m^*. If one assumes $m^*\sim 3-4m_e$, as was found for LSCO and YBCO systems, the superfluid density inferred from the optimally doped Bi2201 becomes about a factor 5–6 smaller than the carrier density $n_{Hall}=1$ per Cu derived in the high-field Hall measurements at $T<1.6$K. In the plot of T_c vs $n_s/m^*(T\rightarrow 0)$, points from the present Bi2201 results lie close to those from the microwave and H_{c1} results of YBCO single crystals which have very reduced $T_c<20$ K, while the points from the inductance measurements of YBCO thin films show much lower superfluid density, off by a factor of 5. In contrast to the cases of LSCO and some other systems, we did not find a signature of field-induced muon-spin relaxation in Bi2201 ($x=0.4$) in a high transverse field of 5 T applied parallel to the c axis. We also described details of the procedure of angular averaging of the penetration depth results of μSR in ceramic specimens having a modest alignment of c-axis orientations.

ACKNOWLEDGMENTS

We acknowledge financial support from NSF DMR-01-02752 and 05-02706 at Columbia, NSERC and CIAR (Canada) at McMaster, NEDO (Japan) at U. Tokyo, and MEXT (Monkashyo) (Japan) Scientific Research (B) and (S) at U. Tokyo. The crystal growth work at Stanford University was supported by DOE under Contracts No. DE-FG03-99ER45773 and No. DE-AC03-76SF00515. The work at Columbia University was partially supported also by the Nanoscale Science and Engineering Initiative of NSF CHE-0117752 and by the New York State Office of Science, Technology, and Academic Research (NYSTAR). We also thank Philip Kim for taking the SEM image shown in Fig. 8.

*Present address: TRIUMF, 4004 Wesbrook Mall, Vancouver, B.C., Canada V6T 2A3.

†Present address: Department of Physics and NHMFL, Florida State University, Tallahassee, Florida 32310-4005.

‡Author to whom correspondence should be addressed. Email address: tomo@lorentz.phys.columbia.edu

§Present address: National Metrology Institute of Japan, AIST, Tsukuba 305-8568, Japan.

‖Present address: Nanoelectronic Research Institute, AIST, Tsukuba 305-8568, Japan.

[1] Y. J. Uemura, Physica B **374-375**, 1 (2006).

[2] Y. J. Uemura, J. Phys.: Condens. Matter **16**, S4515 (2004).

[3] Y. J. Uemura, G. M. Luke, B. J. Sternlieb, J. H. Brewer, J. F. Carolan, W. N. Hardy, R. Kadono, J. R. Kempton, R. F. Kiefl, S. R. Kreitzman, P. Mulhern, T. M. Riseman, D. Ll. Williams, B. X. Yang, S. Uchida, H. Takagi, J. Gopalakrishnan, A. W. Sleight, M. A. Subramanian, C. L. Chien, M. Z. Cieplak, Gang Xiao, V. Y. Lee, B. W. Statt, C. E. Stronach, W. J. Kossler, and X. H. Yu, Phys. Rev. Lett. **62**, 2317 (1989).

[4] Y. J. Uemura, L. P. Le, G. M. Luke, B. J. Sternlieb, W. D. Wu, J. H. Brewer, T. M. Riseman, C. L. Seaman, M. B. Maple, M. Ishikawa, D. G. Hinks, J. D. Jorgensen, G. Saito, and H. Yamochi, Phys. Rev. Lett. **66**, 2665 (1991).

[5] B. Nachumi, A. Keren, K. Kojima, M. Larkin, G. M. Luke, J. Merrin, O. Tchernyshov, Y. J. Uemura, N. Ichikawa, M. Goto, and S. Uchida, Phys. Rev. Lett. **77**, 5421 (1996).

[6] A. T. Savici, Y. Fudamoto, I. M. Gat, T. Ito, M. I. Larkin, Y. J. Uemura, G. M. Luke, K. M. Kojima, Y. S. Lee, M. A. Kastner, R. J. Birgeneau, and K. Yamada, Phys. Rev. B **66**, 014524 (2002).

[7] K. M. Kojima, S. Uchida, Y. Fudamoto, I. M. Gat, M. I. Larkin, Y. J. Uemura, and G. M. Luke, Physica B **326**, 316 (2003).

[8] Y. J. Uemura, A. Keren, L. P. Le, G. M. Luke, W. D. Wu, Y. Kubo, T. Manako, Y. Shimakawa, M. Subramanian, J. L. Cobb, and J. T. Markert, Nature (London) **364**, 605 (1993).

[9] Y. J. Uemura, Solid State Commun. **120**, 347 (2001).

[10] B. Pümpin, H. Keller, W. Kündig, I. M. Savić, J. W. Schneider, H. Simmer, P. Zimmermann, E. Kaldis, S. Rusiecki, and C. Rossel, Hyperfine Interact. **63**, 25 (1990).

[11] C. L. Seaman, J. J. Neumeier, M. B. Maple, L. P. Le, G. M. Luke, B. J. Sternlieb, Y. J. Uemura, J. H. Brewer, R. Kadono, R. F. Kiefl, S. R. Kreitzman, and T. M. Riseman, Phys. Rev. B **42**, 6801 (1990).

[12] J. L. Tallon, C. Bernhard, U. Binninger, A. Hofer, G. V. M. Williams, E. J. Ansaldo, J. I. Budnick, and Ch. Niedermayer, Phys. Rev. Lett. **74**, 1008 (1995).

[13] Ch. Niedermayer, C. Bernhard, U. Binninger, H. Glückler, J. L. Tallon, E. J. Ansaldo, and J. I. Budnick, Phys. Rev. Lett. **71**, 1764 (1993).

[14] A. Keren, A. Kanigel, J. S. Lord, and A. Amato, Solid State Commun. **126**, 39 (2003).

[15] C. Bernhard, J. L. Tallon, Th. Blasius, A. Golnik, and Ch. Niedermayer, Phys. Rev. Lett. **86**, 1614 (2001).

[16] J. Hofer, J. Karpinski, M. Willemin, G. I. Meijer, E. M. Kopnin, R. Molinski, H. Schwer, C. Rossel, and H. Keller Physica C **297**, 103–110 (1998).

[17] P. Nozières and S. Schmitt-Rink, J. Low Temp. Phys. **59**, 195 (1985).

[18] Y. J. Uemura, *Proceedings of the International Workshop on Polarons and Bipolarons in High-T_c, Superconductors and Related Materials, Cambridge, UK, April, 1994*, edited by E. Salje, A. S. Alexandrov, and Y. Liang (Cambridge University Press, Cambridge, England, 1995), pp.453–460.

[19] Y. J. Uemura, *Proceedings of International Symposium/Workshop on High-T_c, Superconductivity and the* C_{60}, *Family, May 1994, Beijing*, edited by H. C. Ren (Gordon and Breach, New York, 1995), pp. 113–142.

[20] Y. J. Uemura, Physica C **282–287**, 194 (1997).

[21] M. Randeria, *Crossover from BCS theory to Bose-Einstein Condensation, in Bose-Einstein Condensation*, edited by A. Griffin, D. W. Snoke, S. Stringari (Cambridge University Press, Cambridge, England, 1995), pp. 355–391, and references therein.

[22] P. A. Lee and N. Nagaosa, Phys. Rev. B **46**, 5621 (1992).

[23] P. A. Lee and X. G. Weng, Phys. Rev. Lett. **78**, 4111 (1997).

[24] R. Friedberg and T. D. Lee, Phys. Rev. B **40**, 6745 (1989).

[25] R. Friedberg, T. D. Lee, and H. C. Ren, Phys. Lett. A **152**, 423 (1991).

[26] S. Doniach and M. Inui, Phys. Rev. B **41**, 6668 (1990).

[27] V. Emery and S. Kivelson, Nature (London) **374**, 434 (1995).

[28] T. Schneider, Z. Phys. B: Condens. Matter **88**, 249 (1992).

[29] T. Schneider and H. Keller, Int. J. Mod. Phys. B **8**, 487 (1993).

[30] T. Schneider and H. Keller, New J. Phys. **6**, 144 (2004).

[31] Y. Ando, G. S. Boebinger, A. Passner, T. Kimura, and K. Kishio, Phys. Rev. Lett. **75**, 4662 (1995).

[32] Y. Ando, G. S. Boebinger, A. Passner, N. L. Wang, C. Geibel, and F. Steglich, Phys. Rev. Lett. **77**, 2065 (1996).

[33] G. S. Boebinger, Y. Ando, A. Passner, T. Kimura, M. Okuya, J. Shimoyama, K. Kishio, K. Tamasaku, N. Ichikawa, and S. Uchida, Phys. Rev. Lett. **77**, 5417 (1996).

[34] F. F. Balakirev, J. B. Betts, A. Migliori, S. Ono, Y. Ando, and G. S. Boebinger, Nature (London) **424**, 912 (2003).

[35] Y. Ando and T. Murayama, Phys. Rev. B **60**, R6991 (1999).

[36] S. Ono, Y. Ando, T. Murayama, F. F. Balakirev, J. B. Betts, and G. S. Boebinger, Phys. Rev. Lett. **85**, 638 (2000).

[37] Y. Ando, S. Ono, X. F. Sun, J. Takeya, F. F. Balakirev, J. B. Betts, and G. S. Boebinger, Phys. Rev. Lett. **92**, 247004 (2004).

[38] R. Liang, D. A. Bonn, W. N. Hardy, and D. Broun, Phys. Rev. Lett. **94**, 117001 (2005).

[39] D. M. Broun, P. J. Turner, W. A. Huttema, S. Ozcan, B. Morgan, R. Liang, W. N. Hardy, and D. A. Bonn, cond-mat/0509223 (unpublished).

[40] Yu. Zuev, M. S. Kim, and T. R. Lemberger, Phys. Rev. Lett. **95**, 137002 (2005).

[41] S. Sanna, G. Allodi, G. Concas, A. D. Hillier, and R. De Renzi, Phys. Rev. Lett. **93**, 207001 (2004).

[42] S. L. Lee, in *Proceedings of the Fifty First Scottish Universities Summer School in Physics, St. Andrews, 1998*, edited by S. L. Lee, S. H. Kilcoyne, and R. Cywinski (Institute of Physics Publishing, Bristol, 1999), p. 149.

[43] S. L. Lee, P. Zimmermann, H. Keller, M. Warden, I. M. Savic, R. Schauwecker, D. Zech, R. Cubitt, E. M. Forgan, P. H. Kes, T. W. Li, A. A. Menovsky, and Z. Tarnawski, Phys. Rev. Lett. **71**, 3862 (1993).

[44] D. R. Harshman, R. N. Kleiman, M. Inui, G. P. Espinosa, D. B. Mitzi, A. Kapitulnik, T. Pfiz, and D. Ll. Williams, Phys. Rev. Lett. **67**, 3152 (1991).

[45] A. T. Savici, A. Fukaya, I. M. Gat-Malureanu, T. Ito, P. L. Russo, Y. J. Uemura, C. R. Wiebe, P. P. Kyriakou, G. J. MacDougall, M. T. Rovers, G. M. Luke, K. M. Kojima, M. Goto, S. Uchida, R. Kadono, K. Yamada, S. Tajima, T. Masui, H. Eisaki, N. Kaneko, M. Greven, and G. D. Gu, Phys. Rev. Lett. **95**, 157001 (2005).

[46] Z. A. Xu, N. P. Ong, Y. Wang, T. Kakeshita, and S. Uchida, Nature (London) **406**, 486 (2000).

[47] Y. Wang, S. Ono, Y. Onose, G. Gu, Y. Ando, Y. Tokura, S. Uchida, and N. P. Ong, Science **299**, 86 (2003).

[48] Y. Wang, Z. A. Xu, T. Kakeshita, S. Uchida, S. Ono, Y. Ando, and N. P. Ong, Phys. Rev. B **64**, 224519 (2001).

[49] Y. Wang, Lu Li, M. J. Naughton, G. D. Gu, S. Uchida, and N. P. Ong, Phys. Rev. Lett. **95**, 247002 (2005).

[50] P. W. Anderson, Phys. Rev. Lett. **96**, 017001 (2006).

[51] For general aspects and historical development of μSR, see Proceedings of ten International Conferences on Muon Spin

Rotation/Relaxation/Resonance in Hyperfine Interact. **6** (1979); **8** (1981); **17-19** (1984); **31** (1986); **63-65** (1990); **85-87** (1994); **104-106** (1997); Physica B **289-290** (2000); **326** (2003); **374-375** (2006).

[52] For recent reviews of μSR studied in strongly correlated electron systems, see Special Issue of μSR, J. Phys.: Condens. Matter **16**, S4403 (2004).

[53] For reviews of μSR and relevant studies in high-T_c cuprate systems, see *Proceedings of the High-T_c Superconductivity Workshop, Williamsburg, Virginia, 2002*, edited by A. J. Millis, S. Uchida, and Y. J. Uemura [Solid State Commun. **126**, 1 (2003)].

[54] For a general review of μSR, see, for example, A. Schenck, *Muon Spin Rotation Spectroscopy* (Adam Hilger, Bristol, 1985).

[55] For a recent reviews of μSR studies in topical subjects, see *Proceedings of the Fifty First Scottish Universities Summer School in Physics, St. Andrews, August, 1988*, edited by S. L. Lee, S. H. Kilcoyne, and R. Cywinski (Inst. of Physics Publishing, Bristol, 1999).

[56] J. H. Brewer and R. Cywinsky, in *Proceedings of the Fifty First Scottish Universities Summer School in Physics* (Ref. 55), pp. 1–8, Fig. 1.

[57] R. F. Kiefl, J. H. Brewer, I. Affleck, J. F. Carolan, P. Dosanjh, W. N. Hardy, T. Hsu, R. Kadono, J. R. Kempton, S. R. Kreitzman, Q. Li, A. H. OŔeilly, T. M. Riseman, P. Schleger, P. C. E. Stamp, H. Zhou, L. P. Le, G. M. Luke, B. Sternlieb, Y. J. Uemura, H. R. Hart, and K. W. Lay, Phys. Rev. Lett. **64**, 2082 (1990).

[58] J. E. Sonier, J. H. Brewer, and R. F. Kiefl, Rev. Mod. Phys. **72**, 769 (2000).

[59] S. Ono and Y. Ando, Phys. Rev. B **67**, 104512 (2003).

[60] H. Eisaki, N. Kaneko, D. L. Feng, A. Damascelli, P. K. Mang, K. M. Shen, Z.-X. Shen, and M. Greven, Phys. Rev. B **69**, 064512 (2004).

[61] K. Fujita, T. Noda, K. M. Kojima, H. Eisaki, and S. Uchida, Phys. Rev. Lett. **95**, 097006 (2005).

[62] Y. J. Uemura, W. J. Kossler, X. H. Yu, J. R. Kempton, H. E. Schone, D. Opie, C. E. Stronach, D. C. Johnston, M. S. Alvarez, and D. P. Goshorn, Phys. Rev. Lett. **59**, 1045 (1987).

[63] See, for example, Fig. 2 of P. Zimmermann, H. Keller, S. L. Lee, I. M. Savic, M. Warden, D. Zech, R. Cubitt, E. M. Forgan, E. Kaldis, J. Karpinski, and C. Krüger, Phys. Rev. B **52**, 541 (1995).

[64] R. I. Grynszpan, P. L. Langlois, D. R. Noakes, C. E. Stronach, M. M. Granderson, E. J. Ansaldo, J. R. Brownstein, A. J. Hill, and T. J. Bastow, Hyperfine Interact. **105**, 95 (1997).

[65] W. Barthord and J. M. F. Gunn, Physica C **156**, 515 (1988).

[66] E. M. Forgan, S. L. Lee, S. Sutton, J. S. Abell, S. F. J. Cox, C. A. Scott, H. Keller, B. Pumpin, J. W. Schneider, H. Simmler, P. Zimmermann, and I. M. Savic, Hyperfine Interact. **63**, 71 (1990).

[67] C. M. Aegerter, S. L. Lee, H. Keller, E. M. Forgan, and S. H. Lloyd, Phys. Rev. B **54**, R15661 (1996).

[68] M. Weber, A. Amato, F. N. Gygax, A. Schenck, H. Maletta, V. N. Duginov, V. G. Grebinnik, A. B. Lazarev, V. G. Olshevsky, V. Yu. Pomjakushin, S. N. Shilov, V. A. Zhukov, B. F. Kirillov, A. V. Pirogov, A. N. Ponomarev, V. G. Storchak, S. Kapusta, and J. Bock, Phys. Rev. B **48**, 13022 (1993).

[69] Y. J. Uemura, A. Keren, G. M. Luke, L. P. Le, B. J. Sternlieb, W. D. Wu, J. H. Brewer, R. L. Whetten, S. M. Huang, Sophia Lin, R. B. Kaner, F. Diederich, S. Donnovan, G. Grüner, and K. Holczer, Nature (London) **352**, 605 (1991).

[70] J. E. Sonier, R. F. Kiefl, J. H. Brewer, D. A. Bonn, S. R. Dunsiger, W. N. Hardy, R. Liang, W. A. MacFarlane, T. M. Riseman, D. R. Noakes, and C. E. Stronach, Phys. Rev. B **55**, 11789 (1997).

[71] J. E. Sonier, J. H. Brewer, R. F. Kiefl, D. A. Bonn, S. R. Dunsiger, W. N. Hardy, R. Liang, W. A. MacFarlane, R. I. Miller, T. M. Riseman, D. R. Noakes, C. E. Stronach, and M. F. White Jr., Phys. Rev. Lett. **79**, 2875 (1997).

[72] J. E. Sonier, J. H. Brewer, R. F. Kiefl, D. A. Bonn, J. Chakhalian, S. R. Dunsiger, W. N. Hardy, R. Liang, W. A. MacFarlane, R. I. Miller, D. R. Noakes, T. M. Riseman, and C. E. Stronach, Phys. Rev. B **61**, R890 (2000).

[73] Ø. Fisher, J. M. Triscone, O. Brunner, L. Antognazza, M. Affronte, O. Eibt, L. Miéville, T. Boichat, and M. G. Karkut, Physica B **169**, 116 (1991).

[74] W. J. Padilla, Y. S. Lee, M. Dumm, G. Blumberg, S. Ono, K. Segawa, S. Komiya, Y. Ando, and D. N. Basov, Phys. Rev. B **72**, 060511(R) (2005).

[75] Y. Ando, N. Balakirev, and G. Boebinger (private communication).

[76] N. P. Ong, Phys. Rev. B **43**, 193 (1991).

[77] K. M. Lang, V. Madhavan, J. E. Hoffman, E. W. Hudson, H. Eisaki, S. Uchida, and J. C. Davis, Nature (London) **415**, 412–416 (2002).

[78] K. McElroy, D.-H. Lee, J. E. Hoffman, K. M. Lang, J. Lee, E. W. Hudson, H. Eisaki, S. Uchida, and J. C. Davis, Phys. Rev. Lett. **94**, 197005 (2004).

[79] J. M. Kosterlitz and D. J. Thouless, J. Phys. C **6**, 1181 (1973).

[80] Y. Sidis, S. Pailhés, B. Keimer, P. Bourges, C. Ulrich, and L. P. Regnault, Phys. Status Solidi B **241**, 1204 (2004), and references therein.

[81] Y. Gallais, A. Sacuto, P. Bourges, Y. Sidis, A. Forget, and D. Colson, Phys. Rev. Lett. **88**, 177401 (2002), and references therein.

[82] A. Damascelli, Z. Hussain, and Z. X. Shen, Rev. Mod. Phys. **75**, 473 (2003) (see Fig. 50 on p. 513).

[83] O. W. Dietrich, E. H. Graf, C. H. Huang, and L. Passell,Phys. Rev. A **5**, 1377 (1972).

[84] N. B. Christensen, D. F. McMorrow, H. M. Rønnow, B. Lake, S. Hayden, G. Aeppli, T. G. Perring, M. Mangkorntong, M. Nohara, and H. Takagi, Phys. Rev. Lett. **93**, 147002 (2004).

[85] N. P. Ong (private communications).